CFD Letters 15, Issue 4 (2023) 114-131

CFD Letters

Journal homepage:
https://semarakilmu.com.my/journals/index.php/CFD_Letters/index
ISSN: 2180-1363

Analytical Treatment for Accelerated Riga Plate on Fractional Caputo-Fabrizio Casson Fluid

Ridhwan Reyaz[1], Ahmad Qushairi Mohamad[1,*], Yeou Jiann Lim[1], Sharidan Shafie[1]

[1] Department of Mathematical Sciences, Faculty of Science, Universiti Teknoogi Malaysia, 81310 Johor Bahru, Johor, Malaysia

ARTICLE INFO

Article history:
Received 6 September 2022
Received in revised form 8 October 2022
Accepted 9 November 2022
Available online 1 April 2023

Keywords:
Caputo-Fabrizio fractional derivative; unsteady Casson fluid flow; Riga plate; Laplace transform

ABSTRACT

The Riga plate is a substantial alteration in the world of engineering. Mainly used in submarines to regulate water flow, studying the behaviour of fluid flowing over a Riga plate is very advantageous. Although there are ample studies on fluid flowing over a Riga plate, the introduction of fractional derivatives, coupled with a non-Newtonian fluid, has yet to be done. Within the field of fluid mechanics, specifically boundary layer flow, fractional derivatives do not have a proven geometrical representation. However, analytical solutions would be useful in aiding experimental researches in the future. Thus, this study aims to present an analytical function for a Caputo-Fabrizio fractional derivative on an unsteady Casson fluid flowing over an accelerating vertical Riga plate by using the Laplace transform method. The parametric effects considered in this study is elucidated. Through observation of obtained graphical results generated via the obtained analytical solutions, it is found that amplification of the fractional parameter and modified Hartmann number increases the fluid velocity with an average increment of 42.05% and 1.56%, respectively. While amplification of the Casson parameter and Prandtl number dampens the fluid velocity by an average of 45.09% and 43.56%, respectively.

1. Introduction

Introduced by Gailitis and Lielausis [1], the Riga plate is an actuator built by stacking together electrodes and magnets of the same size together side by side. Due to its electromagnetichydrodynamic (EMHD) properties, Riga plates are able to generate a Lorentz force. Changing the position of the Riga plate, the Lorentz force generated would either aid or hinder fluid flow. Making Riga plates very convenient as a medium in controlling fluid flow. It is often used in submarines to reduce drag flow and turbulence [2]. Modelling fluid flowing over a Riga plate generates the Grinberg term in the governing momentum equation. Through the process of non-dimensionalisation, the Grinberg term is reduced to a term with the modified Hartmann number as its coefficient [3]. Evaluation of the Riga plate is done through observing the effects of the modified Hartmann number on fluid flow.

* *Corresponding author.*
E-mail address: ahmadqushairi@utm.my (Ahmad Qushairi Mohamad)

https://doi.org/10.37934/cfdl.15.4.114131

Early works of fluid flow over a Riga plate includes Loganathan and Deepa [4, 5] and Loganathan and Dhivya [6] where authors considered Casson fluid flowing over a Riga plate. Each study considered different effects applied on the fluid flow, but all of them flows over a Riga plate. Authors noted that with an increase in the modified Hartmann number, the fluid velocity increases. This is due to the position of the Riga plate, where the Lorentz force generated are parallel to fluid flow, aiding it and increasing its velocity. Later, the study was replicated by Nasrin *et al.,* [7] by considering a rotating Casson fluid and the result, with regards to the modified Hartmann number, were in accordance to that of Loganathan *et al.,* [4–6, 8]. Other works on fluid flow over Riga plates includes Shah *et al.,* [9], Rizwana *et al.,* [10], Mallawi *et al.,* [11] and Khatun *et al.,* [12]. The study of Riga plates is very diverse. Nanofluids, fluid containing nano-sized particles in, were also considered when investigating fluid flow over a Riga plate. Bhatti and Micaelides [13] investigated the Arrhenius activation energy of a nanofluid over a Riga plate. Abbas *et al.,* [14] studied mixed convection flow of Casson nanofluid over a Riga plate. Other studies on nanofluids include Prasad *et al.,* [15], Waini *et al.,* [16], Waini *et al.,* [17] and Khashi'ie *et al.,* [18].

Most of the literature mentioned above solved their problems through a numerical approach. Exact or analytical solutions on fluid flowing over a Riga plate is very scarce. Furthermore, none of the literature considered fractional derivatives in their studies. Fractional derivatives have been proven to produce a spectrum of solutions, providing more options for experimental and numerical researchers to validate their studies. Even though the geometrical representations of fractional derivatives have yet to be found, the analytical solutions will be very beneficial to future researchers to validate their studies.

The Caputo fractional derivative was first introduced into an unsteady Casson fluid flow over a vertical plate by Khan *et al.,* [19]. The Laplace transform of Caputo's fractional derivative contains frequency domain parameter with powers of α. Special functions called the Mittag-Lefler and Wright function is generated from analytically solving a function with the Caputo fractional derivative. Authors presented the boundary layer problem solution in terms of Wright function and proceeded to plot the solution via numerical method of inverse Laplace transform. This would indicate that the final analytical solution presented as a smidgen impractical in terms of future experimental studies. Another effect considered in the study is an exponentially accelerated plate. Ali *et al.,* [20], extended the same study by considering an oscillating plate. Outcome of the study were complimentary to that of Khan *et al.,*[19]. Another approach to solving the Caputo fractional derivative was showcased by Khan *et al.,* [21]. The method involves transforming the equation using Laplace transform, solving the ODE and finally Laplace inverse suing Zakian's method. This approach is considered as a semi-analytical approach instead of an analytical approach due to the nonexistence of a final analytical solution. The semi-analytical approach is an excellent alternative in solving complicated problems such as the one considered by Khan *et al.,* [21], where fluid flow was considered to be in a channel.

Another definition of fractional derivative is known as the Caputo-Fabrizio fractional derivative. Based on the decay exponential law, the fractional operator of the Caputo-Fabrizio fractional derivative does not contain a singular kernel [22]. Essentially, when solving the Caputo-Fabrizio fractional derivative via Laplace transform and Laplace inverse transform, the final solutions are presented as a linear integral function without any special functions. Making it easier to compute since special functions tend to have singularities and is indefinite for certain values of y. A comparative study by Sheikh *et al.,* [23,24] suggested that boundary value problems, where the Caputo-Fabrizio fractional derivative is considered, are able to generate a final analytical solution that is map-able onto a graphical solution. It is also shown that different definitions, carries different analytical solutions and produces different numerical values. Another study by Jamil *et al.,* [25] explored the Caputo-Farbizio fractional derivative on a Casson model for blood flow within a multistenosed artery at an incline. Utilising both the Laplace and Hankel transform, governing equations are solved analytically and obtained solutions suggests that velocity of fluid were amplified with an increase in the Casson parameter and Reynold's number. However, with the increment of the Hartmann number, the velocity of the fluid was dampened. A similar study was done by Maiti *et al.,* [26] showcased similar findings.

To the best of authors knowledge, up to now, there are no analytical studies on the Caoputo-Fabrizio fractional derivatives on Casson fluid flow over an accelerated Riga plate. The aim of this study is to produce analytical solutions for a Caputo-Fabrizio fractional derivative for an unsteady Casson fluid flow over an accelerating Riga plate by utilising the Laplace and Laplace inverse transform method. Novelties of this study includes:

i. Introducing an accelerated Riga plate to an existing unsteady Casson fluid flow problem.
ii. Introducing the Caputo-Fabrizio fractional derivative into an unsteady Casson fluid flow over a accelerated Riga plate.
iii. Providing analytical solutions for an unsteady Casson fluid flow over a accelerated Riga plate with Caputo-Fabrizio fractional derivative.

Parametric evaluation on obtained solutions, including the skin friction and Nusselt number, are also elucidated.

2. Mathematical Formulation

An unsteady free convection flow of a Casson fluid past a semi-infinite vertical Riga plate is considered. The x -axis is taken along the Riga plate in the vertical direction and the y -axis is taken normal to the plate. The fluid is considered to be flowing along the x -direction and to only occupy the space of $y > 0$. Initially, both the fluid and the plate are at rest and their temperature is T_∞, the ambient temperature. When $t > 0$, the plate begins to move and accelerates in the x -direction, against the gravitational field, at the rate of At. Where A is the acceleration of the plate. Meanwhile, the temperature of the plate is raised to T_W and remained constant thereafter. The electromagnetic field induced from the Riga plate, generates an upthrust Lorentz force, F. The Reynold number is assumed to be very minute. Therefore, the magnetic field induced by the movement of the fluid is negligible. A permeated uniform thermal radiation, q_r parallel to the x -axis is applied to the fluid. Velocity, U and temperature, T are dependent on space variable, y and time, t. Figure 1 shows a geometrical representation of the fluid flow and an example of a Riga plate is shown in Figure 2.

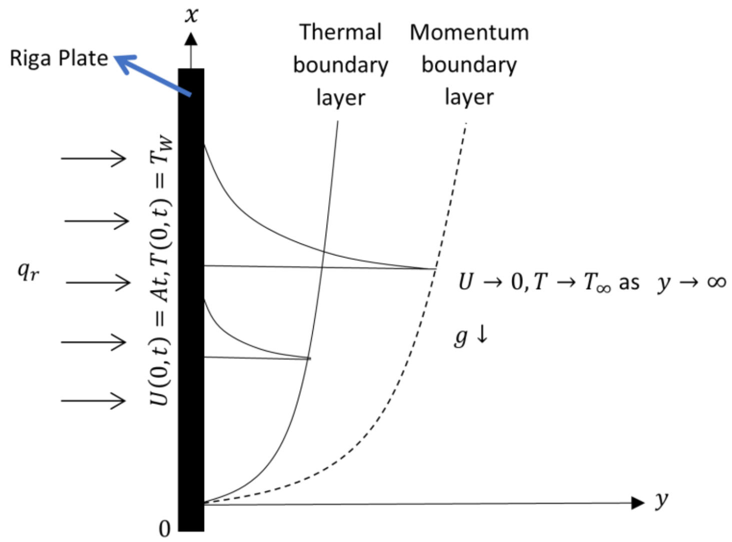

Fig. 1. Physical representation of a free convection flow of a Casson fluid flow

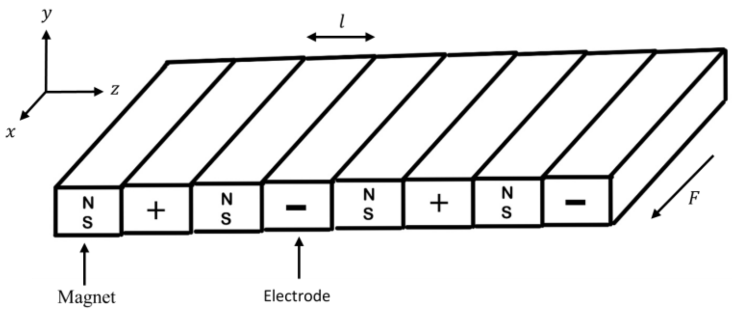

Fig. 2. Riga plate

Based on these assumptions and taking the Boussinesq's approximation into consideration, the governing momentum and energy equations are written as [27-31]

$$\frac{\partial U(y,t)}{\partial t} = \upsilon\left(1+\frac{1}{\beta}\right)\frac{\partial^2 U(y,t)}{\partial y^2} + g\beta_T(T-T_\infty) + \frac{\pi J_0 M_0}{8\rho}exp\left(-\frac{\pi}{l}y\right), \tag{1}$$

$$\rho C_P\frac{\partial T(y,t)}{\partial t} = k\frac{\partial^2 T(y,t)}{\partial y^2} - \frac{\partial q_r}{\partial y}. \tag{2}$$

Both Eq. (1) and Eq. (2) are bounded by initial and boundary conditions:

$$\begin{aligned} &U(y,0)=0, \quad T(y,0)=T_\infty,\\ &U(0,t)=At, \quad T(0,t)=T_W,\\ &U(\infty,t)\to 0, \quad T(\infty,t)\to T_\infty, \end{aligned} \tag{3}$$

where υ is the kinematic viscosity, β is the Casson fluid parameter, g is the gravitational acceleration, β_T is the thermal expansion coefficient, J_0 is the density of electrical current, M_0 the magnitude of magnetization of magnets, ρ is the density of fluid, l is the width of magnets and electrodes of the Riga plate, C_P is the specific heat capacity of the fluid at a constant density, k is the thermal conductivity parameter and q_r is the thermal radiation parameter.

According to Rosseland's approximation [32–34], the governing energy equation from Eq.(2) is reduced to:

$$\rho C_P \frac{\partial T(y,t)}{\partial t} = k \frac{\partial^2 T(y,t)}{\partial y^2} + \frac{16\sigma_1 T_\infty^3}{3k_1}\frac{\partial^2 T(y,t)}{\partial y^2}, \tag{4}$$

where σ_1 is the Stefan-Boltzman constant and k_1 is the mean absorption coefficient.

$$U^* = \frac{U}{(\upsilon A)^{1/3}}, \quad y^* = \frac{yA^{1/3}}{\upsilon^{2/3}}, \quad t^* = \frac{tA^{2/3}}{\upsilon^{1/3}}, \quad T^* = \frac{T - T_\infty}{T_W - T_\infty}, \tag{5}$$

Utilising the dimensionless parameters from Eq. (5) [35–37] and by dropping the asterisk (*) notation, Eq. (1), Eq. (3) and Eq. (4) is further reduced to their dimensionless form such as:

$$\frac{\partial U(y,t)}{\partial t} = \beta_0 \frac{\partial^2 U(y,t)}{\partial y^2} + GrT(y,t) + E\,exp(-Ly), \tag{6}$$

$$\frac{\partial T(y,t)}{\partial t} = \left(1 + \frac{4}{3}N\right)\frac{1}{\mathrm{Pr}}\frac{\partial^2 T(y,t)}{\partial y^2}, \tag{7}$$

bounded by dimensionless initial and boundary conditions:

$$U(y,0) = 0, \quad T(y,0) = 0, \quad U(0,t) = t, \quad T(0,t) = 1, \quad U(\infty,t) \to 0, \quad T(\infty,t) \to 0, \tag{8}$$

where the parameters of β_0, Gr, E, L, N and Pr are defined as:

$$\beta_0 = 1 + \frac{1}{\beta}, \quad Gr = \frac{g\beta_T(T_W - T_\infty)}{A}, \quad E = \frac{\pi J_0 M_0}{8A\rho}, \quad L = \frac{\pi \upsilon^{2/3}}{A^{1/3}l}, \quad N = \frac{4\sigma_1 T_\infty^3}{kk_1}, \quad Pr = \frac{\upsilon\rho C_P}{k}. \tag{9}$$

Here in Eq. (9), β_0 is the dimensionless Casson fluid parameter, Gr is the Grashof number, E is the modified Hartmann number, L is a constant parameter, N is dimensionless thermal radiation parameter and Pr is the Prandtl number.

$$D_t^\alpha f(y,t) = \frac{1}{1-\alpha}\int_0^t \frac{\partial f(y,s)}{\partial y} exp\left(-\alpha\frac{t-s}{1-\alpha}\right) ds. \tag{10}$$

$$\mathcal{L}\{D_t^\alpha f(y,t)\} = \frac{q\bar{f}(y,q) - f(y,0)}{q + \alpha(1-q)}, \tag{11}$$

Eq. (10) and Eq. (11) is the definition of the Caputo-Fabrizio fractional derivative and its respective Laplace transform definition [38–40]. Here, $\mathcal{L}$ denotes the Laplace transform, q denotes the frequency domain and α the fractional derivative parameter.

Replacing the partial derivative with respect to time, $\frac{\partial}{\partial t}$, in Eq. (6) and Eq. (7), with the fractional derivative $D_t^\alpha(\cdot)$, from Eq. (10), converts them into fractional governing momentum and energy equations respectively and can be written as:

$$D_t^{\alpha} U(y,t) = \beta_0 \frac{\partial^2 U(y,t)}{\partial y^2} + GrT(y,t) + E\, exp(-Ly), \tag{12}$$

$$D_t^{\alpha} T(y,t) = \left(1 + \frac{4}{3}N\right) \frac{1}{\Pr} \frac{\partial^2 T(y,t)}{\partial y^2}. \tag{13}$$

3. Analytical Solutions

Obtaining the final analytical solutions was done by first reducing the governing equations from Eq. (12) and Eq. (13) to a frequency domain, q, via the Laplace transform. Using the method of undetermined coefficients and initial and boundary conditions from Eq. (8), solutions of the momentum and energy equations are expressed as:

$$\begin{aligned} \bar{U}(y,q) = &\left[\frac{1}{q^2} - b_1\left(\frac{q+a_1}{q^2}\right) - b_3\left(\frac{q+a_1}{q^2+b_2 q}\right)\right]\exp\left(-y\sqrt{\frac{a_0}{\beta_0}}\sqrt{\frac{q}{q+a_1}}\right) \\ &+ b_1\left(\frac{q+a_1}{q^2}\right)\exp\left(-y\sqrt{\Pr_0 a_0}\sqrt{\frac{q}{q+a_1}}\right) \\ &+ b_3\left(\frac{q+a_1}{q^2+b_2 q}\right)\exp(-Ly), \end{aligned} \tag{14}$$

$$\bar{T}(y,q) = \frac{1}{q}\exp\left(-y\sqrt{\Pr_0 a_0}\sqrt{\frac{q}{q+a_1}}\right). \tag{15}$$

The constant parameters a_0, a_1, b_1, b_2, b_3 and Pr are expressed as:

$$\begin{aligned} &a_0 = \frac{1}{1-\alpha}, \qquad a_1 = \alpha a_0, \\ &b_1 = -\frac{Gr}{\beta_0 \Pr_0 a_0 - a_0}, \quad b_2 = \frac{L^2 \beta_0 a_1}{L^2 \beta_0 - a_0}, \quad b_3 = -\frac{E}{L^2 \beta_0 - a_0}, \\ &\Pr_0 = \frac{\Pr}{1 + \frac{4}{3}N}. \end{aligned} \tag{16}$$

Next, Eq. (14) and Eq. (15) are separated into:

$$\begin{aligned} &\overline{\xi_1}(y,q) = \frac{1}{q^2} - b_1 \overline{\xi_2}(y,q) - b_3 \overline{\xi_3}(y,q), \\ &\overline{\xi_2}(y,q) = \frac{q+a_1}{q^2}, \\ &\overline{\xi_3}(y,q) = \frac{q+a_1}{q^2+b_2 q}, \\ &\overline{\xi_4}(y,q) = \frac{1}{q}, \end{aligned} \tag{17}$$

$$\overline{\psi_1}(y,q) = exp\left(-y\sqrt{\frac{a_0}{\beta_0}}\sqrt{\frac{q}{q+a_1}}\right),$$

$$\overline{\psi_2}(y,q) = exp\left(-y\sqrt{\underset{0}{Pr}a_0}\sqrt{\frac{q}{q+a_1}}\right). \quad (18)$$

Denoting the product of inverse Laplace transform such as:

$$\mathcal{L}^{-1}\{\xi_1(y,q)\} = \xi_1(y,t), \quad \mathcal{L}^{-1}\{\xi_2(y,q)\} = \xi_2(y,t),$$
$$\mathcal{L}^{-1}\{\xi_3(y,q)\} = \xi_3(y,t), \quad \mathcal{L}^{-1}\{\xi_4(y,q)\} = \xi_4(y,t), \quad (19)$$
$$\mathcal{L}^{-1}\{\psi_1(y,q)\} = \psi_1(y,t), \quad \mathcal{L}^{-1}\{\psi_2(y,q)\} = \psi_2(y,t),$$

where $\mathcal{L}^{-1}$ is the notation for inverse Laplace transform. The inverse Laplace transform of Eq. (17) are expressed as:

$$\xi_1(y,t) = t - b_1\xi_2(y,t) - b_3\xi_3(y,t),$$
$$\xi_2(y,t) = 1 + a_1 t,$$
$$\xi_3(y,t) = \frac{a-1}{b_2} + \left(\frac{b_2 - a_1}{b_2}\right) exp(-b_2 t),$$
$$\xi_4(y,t) = 1. \quad (20)$$

Meanwhile, the inverse Laplace transform of Eq. (18) were obtained using the compound function of inverse Laplace transform method and are expressed as [41–43]:

$$\psi_1(y,t) = \int_0^\infty \frac{\sqrt{a_0/\beta_0}}{2\sqrt{\pi}U^{3/2}} exp\left(-\frac{a_0/\beta_0}{4U} - Uy^2 - a_1 t\right)\left[\sqrt{\frac{a_1 U y^2}{t}} I_1\left(2\sqrt{a_1 U y^2 t}\right) + \delta(t)\right] du,$$

$$\psi_2(y,t) = \int_0^\infty \frac{\sqrt{a_0 \underset{0}{Pr}}}{2\sqrt{\pi}U^{3/2}} exp\left(-\frac{a_0 \underset{0}{Pr}}{4U} - Uy^2 - a_1 t\right)\left[\sqrt{\frac{a_1 U y^2}{t}} I_1\left(2\sqrt{a_1 U y^2 t}\right) + \delta(t)\right] du. \quad (21)$$

Here, the notation $I_1(\cdot)$and $\delta(\cdot)$are the modified Bessel function of the first kind of order one and the Dirac delta function, respectively.

Denoted by $U(y,t)$ and $T(y,t)$ the analytical solutions of Eq. (14) and Eq. (15), after they have been inverse Laplace transform, are written in the form of the convolution product such as follows:

$$U(y,t) = \int_0^t \xi_1(y,t-s)\psi_1(y,s)ds + \int_0^t b_1\,\xi_2(y,t-s)\psi_2(y,s)ds + b_3\xi_3(y,t)\,exp(-Ly), \quad (22)$$

$$T(y,t) = \int_0^t \xi_4(y,t-s)\psi_2(y,s)ds. \quad (23)$$

Substituting Eq. (20) and Eq. (21) as well replacing the modified Bessel function with its integral form in Eq. (22) and Eq. (23), the final analytical solutions of the momentum and the energy equations from Eq. (12) and Eq. (13) are written as:

$$U(y,t)=\frac{\exp(-b_2t)}{b_2}\left[b_3\left(a_1-b_2\right)-\left(b_1b_2+a_1b_3+\left(a_1b_1-1\right)b_2t\right)\exp(b_2t)\right]\left[2\Phi(t)-1\right]$$
$$\int_0^\infty\frac{\sqrt{a_0/\beta_0}}{2\sqrt{\pi}U^{3/2}}\exp\left(-\frac{a_0/\beta_0}{4u}-Uy^2\right)du$$
$$+\int_0^\infty\int_0^t\int_0^\pi\frac{1}{\pi}\left[\left(t-s\right)-b_1\left(1+a_1(t-s)\right)-b_3\left(\frac{a_1}{b_2}+\left(\frac{b_2-a_1}{b_2}\right)\exp\left(-b_2(t-s)\right)\right)\right]$$
$$\frac{\sqrt{a_0/\beta_0}}{2\sqrt{\pi}U^{3/2}}\sqrt{\frac{a_1Uy^2}{s}}\cos\left(\theta\right)\exp\left(-\frac{a_0/\beta_0}{4U}-Uy^2-a_1s+(2\sqrt{a_1Uy^2s})\cos(\theta)\right)d\theta dsdu$$
$$+\left(1+a_1t\right)\left[2\Phi(t)-1\right]\int_0^\infty b_1\frac{\sqrt{a_0\,\Pr_0}}{2\sqrt{\pi}U^{3/2}}\exp\left(-\frac{a_0\Pr_0}{4U}-Uy^2\right)du$$
$$+\int_0^\infty\int_0^t\int_0^\pi\frac{1}{\pi}b_1\left(1+a_1(t-s)\right)\frac{\sqrt{a_0\Pr_0}}{2\sqrt{\pi}U^{3/2}}\sqrt{\frac{a_1Uy^2}{s}}\cos(\theta)$$
$$\exp\left(-\frac{a_0\Pr_0}{4U}-Uy^2-a_1s-\left(2\sqrt{a_1Uy^2s}\right)\cos(\theta)\right)$$
$$+b_3\exp\left(-Ly\right)\left[\frac{a-1}{b_2}+\left(\frac{b_2-a_1}{b_2}\right)\exp\left(-b_2t\right)\right], \tag{24}$$

$$T(y,t)=\left[2\Phi(t)-1\right]\int_0^\infty\frac{\sqrt{a_0Pr_0}}{2\sqrt{\pi}u^{3/2}}\exp\left(\frac{-a_0Pr_0}{4u}-uy^2\right)du$$
$$+\int_0^\infty\int_0^t\int_0^\pi\frac{1}{\pi}\frac{\sqrt{a_0Pr_0}}{2\sqrt{\pi}u^{3/2}}\frac{\sqrt{a_1uy^2}}{\sqrt{s}}\cos(\theta) \tag{25}$$
$$\exp\left(\frac{-a_0Pr_0}{4u}-uy^2-a_1s+\left(2\sqrt{a_1uy^2s}\right)\cos(\theta)\right)d\theta dsdu.$$

3.1 Limiting Cases

The skin friction, C_f, and Nusselt number, Nu, for this problem is investigated numerically and graphically by considering the following equations:

$$C_f(y,t)=-\beta_0\left.\frac{\partial U}{\partial y}\right|_{y=0}, \tag{26}$$

$$Nu(y,t)=\left.\frac{\partial T}{\partial y}\right|_{y=0}. \tag{27}$$

Obtained solutions for both the skin friction and Nusselt number will be discussed in the next section.

4. Results and Discussions

Graphical representations of velocity and temperature profiles obtained from Eqn Eq. (24) and Eq. (25) are illustrated in Figure 3-Figure 10. The MathCad-15 software were used to generate these profiles. A numerical validation of obtained results with published results are displayed in Table 1. Using the same approach, numerical validation and solutions of skin friction as well as the Nusselt number is tabulated in Table 2-Table 3. Meanwhile, the corresponding skin friction and Nusselt number graphical solutions against varied y values are shown in Figure 11 and Figure 12.

The velocity profile with variation in the fractional parameter, α, is shown in Figure 3. As observed, as α increases, so does the velocity profile with an average of 42.05% increment with every value of α. As discussed in the Introduction section, geometrical application of fractional derivatives on the mechanics of fluid flow has yet to be discovered. Nonetheless, the obtained analytical solutions in Eq. (24) and Eq. (25) will be crucial in validating future numerical and experimental research. Figure 3 merely demonstrates the behaviour of a Casson fluid flow over an accelerated Riga plate when the Caputo-Fabrizio fractional derivative is considered with variations in the fractional value.

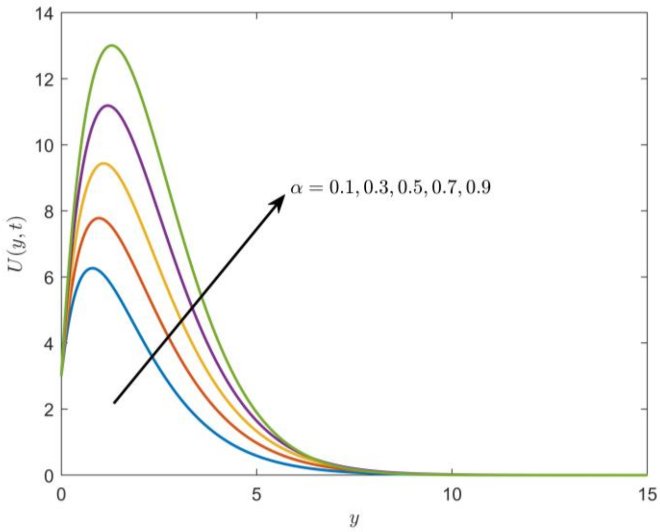

Fig. 3. Velocity of fluid with variations in α when $t = 3$, $\beta = 10$, $Gr = 21$, $Pr = 14$, $N = 9$, $L = 2$, $E = 9$

Meanwhile, Figure 4 shows the velocity profile with variations in the modified Hartman number, E. The modified Hartmann number defines the Riga plate existence. Presence of a Riga plate introduces Lorentz force, into the fluid flow. In this case, the Lorentz force generated is parallel to the fluid flow, increasing the upthrust force experienced by the fluid. Thus, aiding the fluid flow and increasing the velocity of the fluid with an average increment of 1.56%. A large modified Hartmann number signifies a larger Riga plate, which in turns increases the Lorentz force, consequently the fluid velocity.

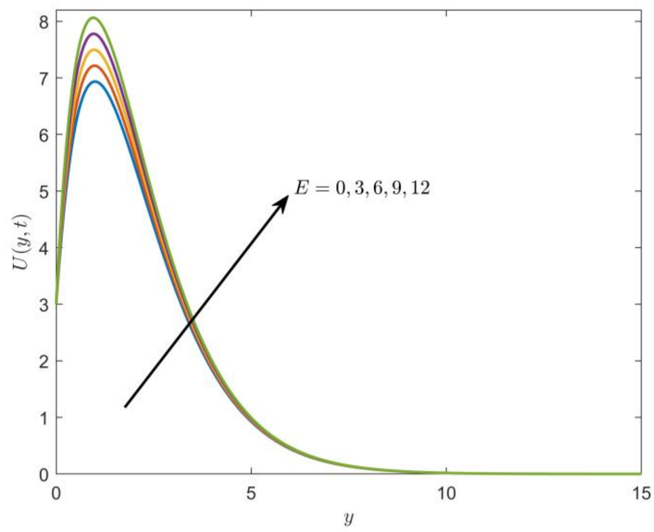

Fig. 4. Velocity of fluid with variations in E when $\alpha = 0.5$, $t = 3$, $\beta = 10$, $Gr = 21$, $Pr = 14$, $N = 9$, $L = 2$

The Casson fluid, a non-Newtonian fluid, is considered in this study. A Casson fluid behaves like a solid when the shear stress is lower than the yield stress, otherwise it exhibits a Newtonian fluid behaviour. It is observed in Figure 5, when $y > 0$ the velocity profile increases with the Casson parameter, β. After a certain point in the y -direction, between 3.2 and 3.4, the velocity profile decreases as β increases. The fluctuation is caused due to the variation in the shear stress. When $0 \leq y \leq 3.2$, shear stress is larger than the yield stress, showcasing a Newtonian fluid behaviour. On the other hand, when $y \geq 3.4$, the shear stress is smaller than the yield stress, increasing the plasticity of the fluid, showcasing a non-Newtonian fluid behaviour. this in turn, decreases the fluid velocity with an average of 45.09% decrement.

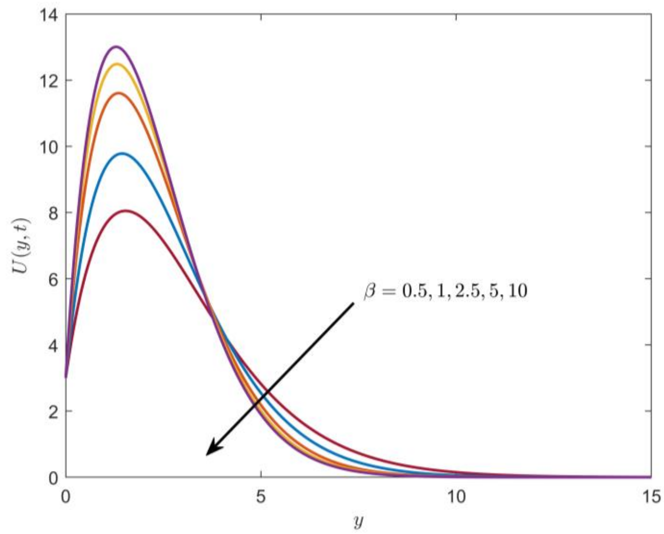

Fig. 5. Velocity of fluid with variations in β when $\alpha = 0.5$, $t = 3$, $Gr = 21$, $Pr = 14$, $N = 9$, $L = 2$, $E = 9$

Concurrently, Figure 6 showcases the velocity profile of the fluid with variations in the Prandtl number, Pr. Pr is the ratio between the momentum diffusivity rate and the heat diffusivity rate. An increase in Pr dampens the heat diffusivity rate, decreasing the kinetic energy in the fluid. Thus, fluid velocity decreases, with an average of 43.56% decrement, with the amplification of the Prandtl number. This is true in this study as observed in Figure 6.

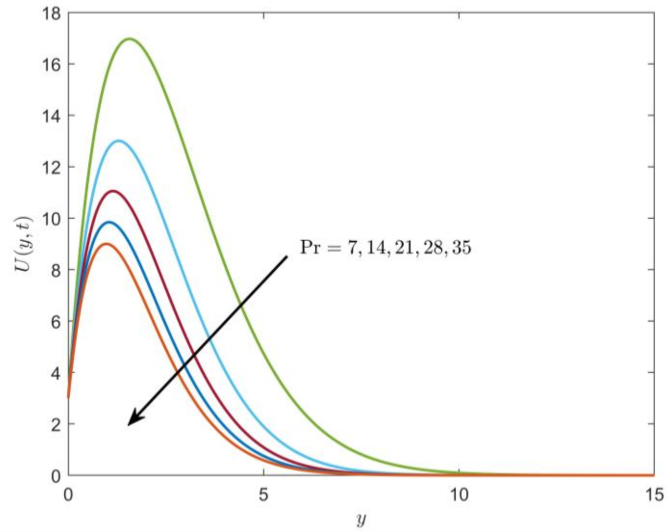

Fig. 6. Velocity of fluid with variations in Pr when $\alpha = 0.5$, $t = 3$, $\beta = 10$, $Gr = 21$, $N = 9$, $L = 2$, $E = 9$

At the same time, Figure 7 showcases the velocity profile of the fluid with variations in the Grashof number, Gr. Gr approximates the ratio between the buoyancy and hydrodynamic viscous force. An increase in Gr amplifies the buoyancy force, increasing the upthrust force experienced by the fluid. Thus, fluid velocity increases with the amplification of the Grashof number with an average increment of 41.72%. This is true for this study as well, as observed in Figure 7.

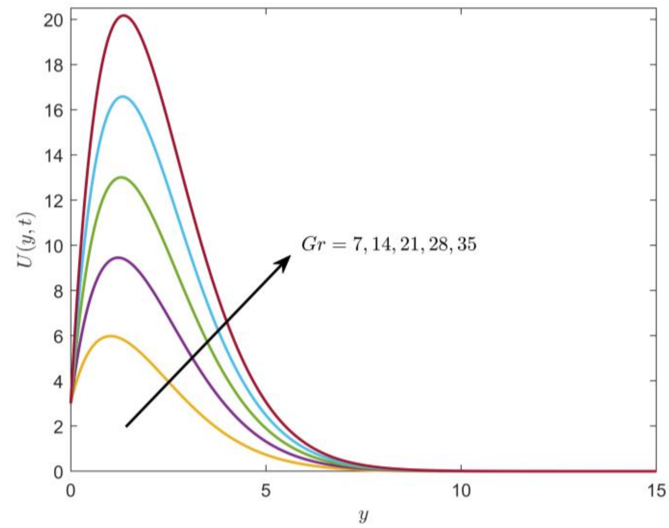

Fig. 7. Velocity of fluid with variations in Gr when $\alpha = 0.5$, $t = 3$, $\beta = 10$, $Pr = 14$, $N = 9$, $L = 2$, $E = 9$

In this study, thermal radiation effect is considered. Radiating heat is introduced to the fluid through the plate. As more heat is introduced, the kinetic energy within the fluid is intensified. Thus, increasing the fluid velocity with an average increment of 76.58%. This behaviour is observed clearly in Figure 8.

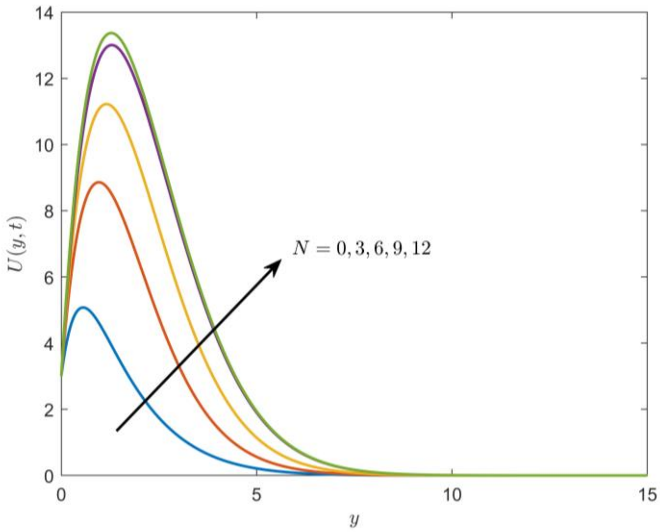

Fig. 8. Velocity of fluid with variations in N when $\alpha = 0.5$, $\beta = 10$, $Gr = 21, Pr = 14, t = 3, L = 2, E = 9$

Figure 9 illustrates the velocity profile with variation in time, t. An accelerating plate is considered in this study. Through the process of non-dimentionalisation, the initial velocity when $y = 0$ is set at t. This is stated in Eq. (8). Variations in t suggests different initial values. This can be observed clearly in Figure 9.

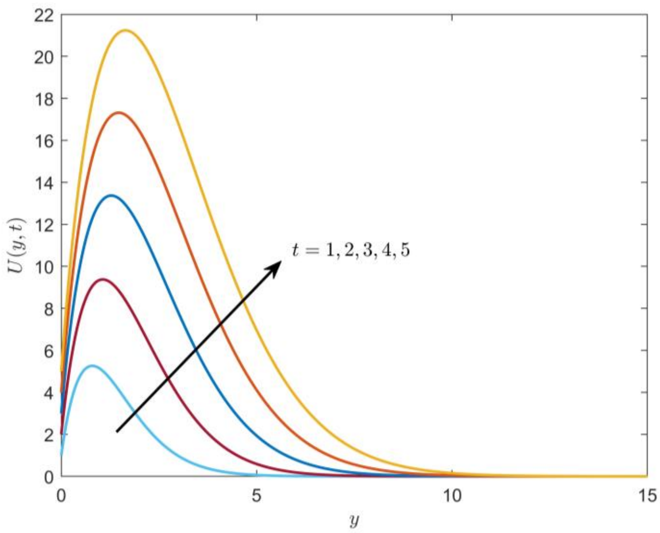

Fig. 9. Velocity of fluid with variations in t when $\alpha = 0.5$, $\beta = 10$, $Gr = 21, Pr = 14, N = 9, L = 2, E = 9$

Both Figure 10 and Figure 11 displays the temperature profiles for the fluid with variations in Pr and N, respectively. The fluid temperature dampens as the value of Pr is increased. As discussed earlier, a decrease in heat diffusivity occurs when the Pr is increased, lowering the kinetic energy of the fluid. Thus, decreasing the fluid temperature, with an average decrement of 73.78%, as observed in Figure 10. Concurrently, the fluid temperature increases, with an average increment of well over 100%, with an increase in N. With some values of y, the increment can even reach up to 300%. With the increase in N, kinetic energy in the fluid is amplified. Thus, increasing the fluid temperature as shown in Figure 11.

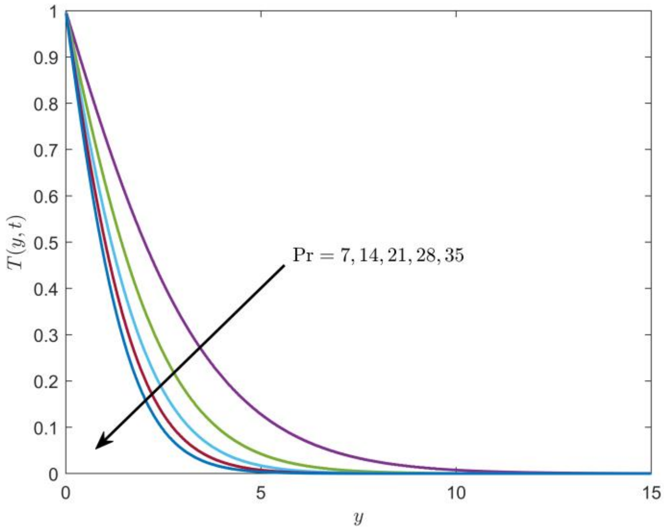

Fig. 10. Temperature of fluid with variations in Pr when $t = 3$, $N = 9$

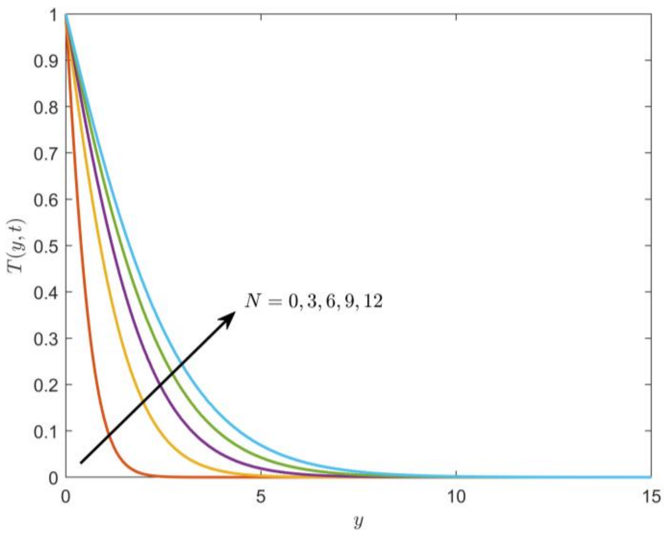

Fig. 11. Temperature of fluid with variations in N when $t = 3$, $Pr = 14$

Table 1 shows the numerical validations of obtained results with published results from Ali *et al.,* [20] and Reyaz *et al.,* [44]. It is observed from the table that the average relative difference from obtained results with that of Ali *et al.,* [20] is 0.27 and 0.44 with Reyaz *et al.,* [44]. These values are due to varied assumptions between current problem and published studies from Ali *et al.,* [20] and Reyaz *et al.,* [44]. For instance, Ali *et al.,* [20] considered the Caputo fractional derivative instead of the Caputo-Fabrizio fractional derivative. Additionally, Reyaz *et al.,* [44] considered mass transfer in their study, however the current study does not. Nonetheless, the relative difference between current study and published study is significantly low. Thus, obtained results from current study is valid.

Table 1
Validation of obtained numerical results with published results

y	Obtained	Ali *et al.,* [20]	Relative Difference	Reyaz *et al.,* [44]	Relative difference
0	1	1	0	1	0
2	0.356000	0.370000	-0.037838	0.341000	0.043988
4	0.052000	0.047000	0.106383	0.042000	0.238095
6	0.007488	0.005858	0.278252	0.005047	0.483654
8	0.001081	0.000722	0.496608	0.000609	0.773876
10	0.000156	0.000088	0.767310	0.000073	1.124147

Table 2 showcases the skin friction, $C_f(y,t)$ at $y=0$, with varied values of α , β , Gr, Pr, E, N and t. These values are obtained by using Eq. (26). It is observed in the third row, that the value for $C_f(y,t)$ decreases by 26.4% when compared to the control values at the first row. This contradicts the properties of a non-Newtonian fluid where the skin friction should have increased when the values of β is increased. However, as discussed previously, since Casson fluid models showcases both properties of Newtonian and non-Newtonian fluid according to the shear stress applied, a decrease in skin friction is plausible. The value also corresponds well with finding from Figure 5. Other than that, the skin friction values correspond well with obtained graphical results from Figure 3-Figure 9.

Table 2
Skin friction, $C_f(y,t)\big|_{y=0}$, coefficient with variations in α, β, Gr, Pr, E, N and t

α	β	Gr	Pr	E	N	t	$C_f(y,t)\big|_{y=0}$	
0.1	0.25	0.3	0.3	3	3	4	6.73	
0.3	0.25	0.3	0.3	3	3	4	5.599	⇓16.81%
0.1	0.5	0.3	0.3	3	3	4	4.953	⇓26.40%
0.1	0.25	0.7	0.3	3	3	4	6.067	⇓9.85%
0.1	0.25	0.3	0.7	3	3	4	6.809	⇑1.17 %
0.1	0.25	0.3	0.3	6	3	4	5.472	⇓18.69%
0.1	0.25	0.3	0.3	3	9	4	6.653	⇓1.14%
0.1	0.25	0.3	0.3	3	3	5	8.566	⇑27.28 %

Table 3 showcases the Nusselt number, $Nu(y,t)$ at $y=0$, with varied values of α , Pr, N and t. These values are obtained using Eq. (27). The Nusselt number showcase the heat transfer rate between the pate and the fluid. According to Table 3, the numbers corresponds well with obtained graphical solutions from Figure 10 and 11.

Table 3
Nusselt number, $Nu(y,t)|_{y=0}$, coefficient with variations in α, Pr, N and t

α	Pr	N	t	$Nu(y,t)|_{y=0}$	
0.1	0.3	3	3	0.22	
0.3	0.3	3	3	0.17	⇓22.72%
0.1	0.7	3	3	0.336	⇑52.72%
0.1	0.3	9	3	0.136	⇓38.18%
0.1	0.3	3	4	0.209	⇓5.00%

Meanwhile, Figure 12 and Figure 13 showcase the skin friction and Nusselt number behaviour with varied values of y. It is shown that the graphical representation of $C_f(y,t)$ and $Nu(y,t)$ is in agreement with both graphical solutions, from Figure 3-Figure 11, as well as numerical solution from Table 2 and Table 3.

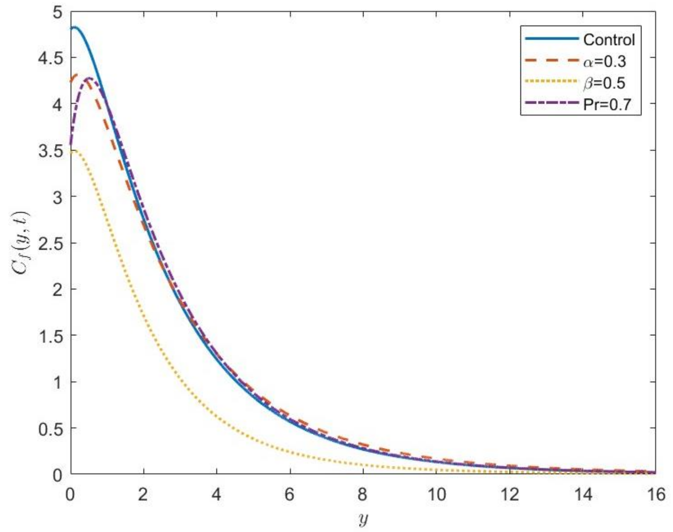

Fig. 12. Skin friction, $C_f(y,t)$, with varied values of α, β and Pr

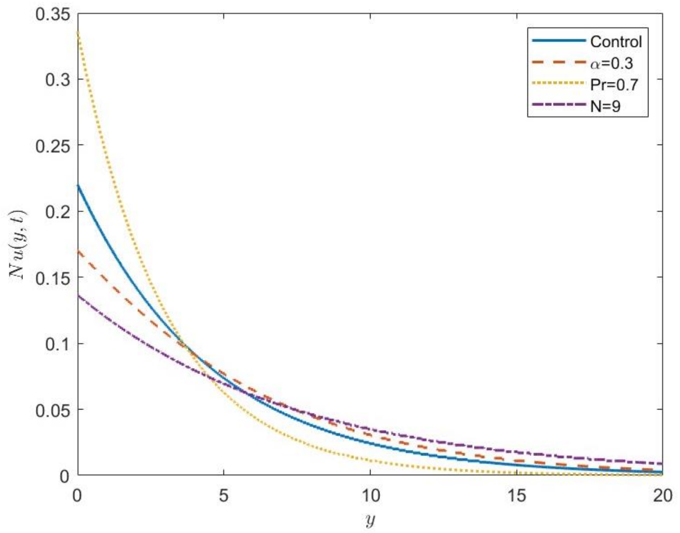

Fig. 13. Nusselt number, $Nu(y,t)$, with varied values of α, Pr and N

5. Conclusions

A study on an unsteady Caputo-Fabrizio fractional Casson fluid flowing over an accelerating Riga plate treated analytically has been done. It is concluded that:

i. An increase in the fractional parameter, α, increases the velocity profile with an average increase of 42.05%.
ii. Amplification in the modified Hartmann number, E, raises the fluid velocity with an average increase of 1.56%.
iii. Fluctuation in the fluid velocity is observed when amplifying the Casson parameter, β. After $y = 3.4$, fluid velocity dampens, with an average of 45.09%.

iv. Amplification in the Prandtl number, Pr , dampens the fluid velocity with an average decrease of 43.56%.
v. Amplification in the Grashof number, Gr, raises fluid velocity with an average increase of 41.72%.
vi. Amplification in the thermal radiation parameter, N, raises the fluid velocity with an average increase of 76.58%.
vii. Amplification in time, t, raises the initial velocity of fluid.
viii. Amplification in the Prandtl number, Pr , dampens the fluid temperature with an average decrease of 73.78%.
ix. Amplification in the thermal radiation parameter, N, raises the fluid temperature.

Acknowledgement
The authors would like to acknowledge the Ministry of Higher Education Malaysia and Research Management Centre-UTM, Universiti Teknologi Malaysia (UTM) for financial support through vote numbers FRGS/1/2019/STG06/UTM/02/22 and 08G33.

References
[1] Khashi'ie, Najiyah Safwa, Norihan Md Arifin, and Ioan Pop. "Mixed convective stagnation point flow towards a vertical Riga plate in hybrid Cu-Al2O3/water nanofluid." *Mathematics* 8, no. 6 (2020): 912. https://doi.org/10.3390/math8060912
[2] Ganesh, N. Vishnu, Qasem M. Al-Mdallal, Sara Al Fahel, and Shymaa Dadoa. "Riga–Plate flow of γ Al2O3-water/ethylene glycol with effective Prandtl number impacts." *Heliyon* 5, no. 5 (2019): e01651. https://doi.org/10.1016/j.heliyon.2019.e01651
[3] Bilal, S., Kanayo K. Asogwa, Hammad Alotaibi, M. Y. Malik, and Ilyas Khan. "Analytical treatment of radiative Casson fluid over an isothermal inclined Riga surface with aspects of chemically reactive species." *Alexandria Engineering Journal* 60, no. 5 (2021): 4243-4253. https://doi.org/10.1016/j.aej.2021.03.015
[4] Loganathan, Parasuraman, and Krishnamurthy Deepa. "Electromagnetic and radiative Casson fluid flow over a permeable vertical Riga-plate." *Journal of Theoretical and Applied Mechanics* 57 (2019). https://doi.org/10.15632/jtam-pl/112421
[5] Loganathan, P., and K. Deepa. "Stratified Casson Fluid Flow Past a Riga-plate with Generative/Destructive Heat Energy." *International Journal of Applied and Computational Mathematics* 6, no. 4 (2020): 1-20. https://doi.org/10.1007/s40819-020-00863-w
[6] Parasuraman, Loganathan, and Deepa Krishnamurthy. "Heat and mass transfer analysis of casson fluid flow on a permeable riga-plate." *Indian Journal of Pure & Applied Physics (IJPAP)* 58, no. 2 (2020): 79-86. https://doi.org/10.1615/InterJFluidMechRes.2020027371
[7] Nasrin, Sonia, Rabindra Nath Mondal, and Md Mahmud Alam. "Impulsively Started Horizontal Riga Plate Embedded in Unsteady Casson Fluid Flow with Rotation." *Journal of Applied Mathematics and Physics* 8, no. 9 (2020): 1861-1876. https://doi.org/10.4236/jamp.2020.89140
[8] Loganathan, Parasuraman, and Krishnamurthy Deepa. "Computational exploration of Casson fluid flow over a Riga-plate with variable chemical reaction and linear stratification." *Nonlinear Analysis: Modelling and Control* 25, no. 3 (2020): 443-460. https://doi.org/10.15388/namc.2020.25.16659
[9] Shah, Faisal, M. Ijaz Khan, Tasawar Hayat, Shaher Momani, and M. Imran Khan. "Cattaneo-Christov heat flux (CC model) in mixed convective stagnation point flow towards a Riga plate." *Computer Methods and Programs in Biomedicine* 196 (2020): 105564. https://doi.org/10.1016/j.cmpb.2020.105564
[10] Rizwana, Rizwana, and S. Nadeem. "Series solution of unsteady MHD oblique stagnation point flow of copper-water nanofluid flow towards Riga plate." *Heliyon* 6, no. 10 (2020): e04689. https://doi.org/10.1016/j.heliyon.2020.e04689
[11] Mallawi, F. O. M., M. Bhuvaneswari, S. Sivasankaran, and S. Eswaramoorthi. "Impact of double-stratification on convective flow of a non-Newtonian liquid in a Riga plate with Cattaneo-Christov double-flux and thermal radiation." *Ain Shams Engineering Journal* 12, no. 1 (2021): 969-981. https://doi.org/10.1016/j.asej.2020.04.010
[12] Khatun, Sheela, Muhammad Minarul Islam, Md Mollah, Saykat Poddar, and Md Alam. "EMHD radiating fluid flow along a vertical Riga plate with suction in a rotating system." *SN Applied Sciences* 3, no. 4 (2021): 1-14. https://doi.org/10.1007/s42452-021-04444-4

[13] Bhatti, M. M., and Efstathios E. Michaelides. "Study of Arrhenius activation energy on the thermo-bioconvection nanofluid flow over a Riga plate." *Journal of Thermal Analysis and Calorimetry* 143, no. 3 (2021): 2029-2038. https://doi.org/10.1007/s10973-020-09492-3

[14] Bhatti, M. M., and Efstathios E. Michaelides. "Study of Arrhenius activation energy on the thermo-bioconvection nanofluid flow over a Riga plate." *Journal of Thermal Analysis and Calorimetry* 143, no. 3 (2021): 2029-2038. https://doi.org/10.1177/0954408917719791

[15] Prasad, Kerehalli Vinayaka, Hanumesh Vaidya, Gudekote Manjunatha, Kuppalapalle Vajravelu, Choudhari Rajashekhar, and V. Ramanjini. "Influence of Variable Transport Properties on Casson Nanofluid Flow over a Slender Riga Plate: Keller Box Scheme." *Journal of Advanced Research in Fluid Mechanics and Thermal Sciences* 64, no. 1 (2019): 19-42.

[16] Waini, Iskandar, Anuar Ishak, and Ioan Pop. "Symmetrical solutions of hybrid nanofluid stagnation-point flow in a porous medium." *International Communications in Heat and Mass Transfer* 130 (2022): 105804. https://doi.org/10.1016/j.icheatmasstransfer.2021.105804

[17] Waini, Iskandar, Umair Khan, Aurang Zaib, Anuar Ishak, and Ioan Pop. "Inspection of TiO2-CoFe2O4 nanoparticles on MHD flow toward a shrinking cylinder with radiative heat transfer." *Journal of Molecular Liquids* 361 (2022): 119615. https://doi.org/10.1016/j.molliq.2022.119615

[18] Khashi'ie, Najiyah Safwa, Iskandar Waini, Nurul Amira Zainal, Khairum Hamzah, and Abdul Rahman Mohd Kasim. "Hybrid nanofluid flow past a shrinking cylinder with prescribed surface heat flux." *Symmetry* 12, no. 9 (2020): 1493. https://doi.org/10.3390/sym12091493

[19] Khan, Ilyas, Nehad Ali Shah, and Dumitru Vieru. "Unsteady flow of generalized Casson fluid with fractional derivative due to an infinite plate." *The European physical journal plus* 131, no. 6 (2016): 1-12. https://doi.org/10.1140/epjp/i2016-16181-8

[20] Ali, Farhad, Nadeem Ahmad Sheikh, Ilyas Khan, and Muhammad Saqib. "Solutions with Wright function for time fractional free convection flow of Casson fluid." *Arabian Journal for Science and Engineering* 42, no. 6 (2017): 2565-2572. https://doi.org/10.1007/s13369-017-2521-3

[21] Khan, Ilyas, Muhammad Saqib, and Farhad Ali. "Application of time-fractional derivatives with non-singular kernel to the generalized convective flow of Casson fluid in a microchannel with constant walls temperature." *The European Physical Journal Special Topics* 226, no. 16 (2017): 3791-3802. https://doi.org/10.1140/epjst/e2018-00097-5

[22] Yépez-Martínez, Huitzilin, and José Francisco Gómez-Aguilar. "A new modified definition of Caputo–Fabrizio fractional-order derivative and their applications to the multi step homotopy analysis method (MHAM)." *Journal of Computational and Applied Mathematics* 346 (2019): 247-260. https://doi.org/10.1016/j.cam.2018.07.023

[23] Sheikh, Nadeem Ahmad, Farhad Ali, Muhammad Saqib, Ilyas Khan, and Syed Aftab Alam Jan. "A comparative study of Atangana-Baleanu and Caputo-Fabrizio fractional derivatives to the convective flow of a generalized Casson fluid." *The European Physical Journal Plus* 132, no. 1 (2017): 1-14. https://doi.org/10.1140/epjp/i2017-11326-y

[24] Sheikh, Nadeem Ahmad, Farhad Ali, Muhammad Saqib, Ilyas Khan, Syed Aftab Alam Jan, Ali Saleh Alshomrani, and Metib Said Alghamdi. "Comparison and analysis of the Atangana–Baleanu and Caputo–Fabrizio fractional derivatives for generalized Casson fluid model with heat generation and chemical reaction." *Results in physics* 7 (2017): 789-800. https://doi.org/10.1016/j.rinp.2017.01.025

[25] Jamil, Dzuliana Fatin, Salah Uddin, M. Ghazali Kamardan, and Rozaini Roslan. "The effects of magnetic blood flow in an inclined cylindrical tube using caputo-fabrizio fractional derivatives." *CFD Letters* 12, no. 1 (2020): 111-122.

[26] Maiti, S., S. Shaw, and G. C. Shit. "Caputo–Fabrizio fractional order model on MHD blood flow with heat and mass transfer through a porous vessel in the presence of thermal radiation." *Physica A: Statistical Mechanics and its Applications* 540 (2020): 123149. https://doi.org/10.1016/j.physa.2019.123149

[27] Asogwa, Kanayo K., Sardar M. Bilal, Isaac L. Animasaun, and Fateh M. Mebarek-Oudina. "Insight into the significance of ramped wall temperature and ramped surface concentration: The case of Casson fluid flow on an inclined Riga plate with heat absorption and chemical reaction." *Nonlinear Engineering* 10, no. 1 (2021): 213-230. https://doi.org/10.1515/nleng-2021-0016

[28] Shahrim, Muhammad Nazirul, Ahmad Qushairi Mohamad, Lim Yeou Jiann, Muhamad Najib Zakaria, Sharidan Shafie, Zulkhibri Ismail, and Abdul Rahman Mohd Kasim. "Exact solution of fractional convective Casson fluid through an accelerated plate." *CFD Letters* 13, no. 6 (2021): 15-25. https://doi.org/10.37934/cfdl.13.6.1525

[29] Hussanan, Abid, Mohd Zuki Salleh, Ilyas Khan, and Razman Mat Tahar. "Heat transfer in magnetohydrodynamic flow of a Casson fluid with porous medium and Newtonian heating." *Journal of nanofluids* 6, no. 4 (2017): 784-793. https://doi.org/10.1166/jon.2017.1359

[30] Reyaz, Ridhwan, Ahmad Qushairi Mohamad, Lim Yeou Jiann, Muhammad Saqib, and Sharidan Shafie. "Presence of Riga Plate on MHD Caputo Casson Fluid: An Analytical Study." *Journal of Advanced Research in Fluid Mechanics and Thermal Sciences* 93, no. 2 (2022): 86-99. https://doi.org/10.37934/arfmts.93.2.8699

[31] Thirupathi, Gurrala, Kamatam Govardhan, and Ganji Narender. "Radiative Magnetohydrodynamics Casson Nanofluid Flow and Heat and Mass Transfer past on Nonlinear Stretching Surface." *Journal of Advanced Research in Numerical Heat Transfer* 6, no. 1 (2021): 1-21.

[32] Zakaria, Muhamad Najib, Abid Hussanan, Ilyas Khan, and Sharidan Shafie. "The effects of radiation on free convection flow with ramped wall temperature in Brinkman type fluid." *Jurnal Teknologi* 62, no. 3 (2013). https://doi.org/10.11113/jt.v62.1886

[33] Anantha Kumar, K., V. Sugunamma, and N. Sandeep. "Effect of thermal radiation on MHD Casson fluid flow over an exponentially stretching curved sheet." *Journal of Thermal Analysis and Calorimetry* 140, no. 5 (2020): 2377-2385. https://doi.org/10.1007/s10973-019-08977-0

[34] Yusof, Nur Syamila, Siti Khuzaimah Soid, Mohd Rijal Illias, Ahmad Sukri Abd Aziz, and Nor Ain Azeany Mohd Nasir. "Radiative Boundary Layer Flow of Casson Fluid Over an Exponentially Permeable Slippery Riga Plate with Viscous Dissipation." *Journal of Advanced Research in Applied Sciences and Engineering Technology* 21, no. 1 (2020): 41-51. https://doi.org/10.37934/araset.21.1.4151

[35] Hussanan, Abid, Mohd Zuki Salleh, Ilyas Khan, and Zhi-Min Chen. "Unsteady water functionalized oxide and non-oxide nanofluids flow over an infinite accelerated plate." *Chinese Journal of Physics* 62 (2019): 115-131. https://doi.org/10.1016/j.cjph.2019.09.020

[36] Khan, Masood, S. Hyder Ali, and Constantin Fetecau. "Exact solutions of accelerated flows for a Burgers' fluid. I. The case γ< λ2/4." *Applied Mathematics and Computation* 203, no. 2 (2008): 881-894. https://doi.org/10.1007/s00033-008-7155-6

[37] Khan, M., S. Hyder Ali, and Haitao Qi. "Some accelerated flows for a generalized Oldroyd-B fluid." *Nonlinear analysis: real world applications* 10, no. 2 (2009): 980-991. https://doi.org/10.1016/j.nonrwa.2007.11.017

[38] Atangana, Abdon, and Dumitru Baleanu. "Caputo-Fabrizio derivative applied to groundwater flow within confined aquifer." *Journal of Engineering Mechanics* 143, no. 5 (2017): D4016005. https://doi.org/10.1061/(ASCE)EM.1943-7889.0001091

[39] Raza, Nauman, and Muhammad Asad Ullah. "A comparative study of heat transfer analysis of fractional Maxwell fluid by using Caputo and Caputo–Fabrizio derivatives." *Canadian Journal of Physics* 98, no. 1 (2020): 89-101. https://doi.org/10.1139/cjp-2018-0602

[40] Asjad, Muhammad Imran, Nehad Ali Shah, Maryam Aleem, and Ilyas Khan. "Heat transfer analysis of fractional second-grade fluid subject to Newtonian heating with Caputo and Caputo-Fabrizio fractional derivatives: A comparison." *The European physical journal plus* 132, no. 8 (2017): 1-19. https://doi.org/10.1140/epjp/i2017-11606-6

[41] Hussanan, Abid, Mohd Zuki Salleh, Ilyas Khan, and Razman Mat Tahar. "Unsteady heat transfer flow of a Casson fluid with Newtonian heating and thermal radiation." *Jurnal Teknologi* 78, no. 4-4 (2016). https://doi.org/10.11113/jt.v78.8264

[42] Hussanan, Abid, Mohd Zuki Salleh, Razman Mat Tahar, and Ilyas Khan. "Unsteady boundary layer flow and heat transfer of a Casson fluid past an oscillating vertical plate with Newtonian heating." *PloS one* 9, no. 10 (2014): e108763. https://doi.org/10.1371/journal.pone.0108763

[43] Mohamad, Ahmad Qushairi, Ilyas Khan, Lim Yeou Jiann, Sharidan Shafie, Zaiton Mat Isa, and Zulkhibri Ismail. "Heat transfer on rotating second grade fluid through an accelerated plate." *Malaysian Journal of Fundamental and Applied Sciences* 13, no. 3 (2017): 219-223. https://doi.org/10.11113/mjfas.v13n3.645

[44] Reyaz, Ridhwan, Ahmad Qushairi Mohamad, Yeou Jiann Lim, Muhammad Saqib, and Sharidan Shafie. "Analytical solution for impact of Caputo-Fabrizio fractional derivative on MHD casson fluid with thermal radiation and chemical reaction effects." *Fractal and Fractional* 6, no. 1 (2022): 38. https://doi.org/10.3390/fractalfract6010038